HHS Public Access

Author manuscript

Stem Cell Res. Author manuscript; available in PMC 2019 December 03.

Published in final edited form as:

Stem Cell Res. 2019 July ; 38: 101470. doi:10.1016/j.scr.2019.101470.

Chemical screen for epigenetic barriers to single allele activation of *Oct4*

Kathryn M. Headley[a,b], **Katarzyna M. Kedziora**[c], **Aidin Alejo**[a], **Elianna Zhi-Xiang Lai**[a], **Jeremy E. Purvis**[b,c,d], **Nathaniel A. Hathaway**[a,b,d,*]

[a]Division of Chemical Biology and Medicinal Chemistry, Center for Integrative Chemical Biology and Drug Discovery, UNC Eshelman School of Pharmacy, Chapel Hill, NC 27599, United States of America

[b]Curriculum for Genetics and Molecular Biology, University of North Carolina, Chapel Hill, NC 27599, United States of America

[c]Department of Genetics, Curriculum for Bioinformatics and Computational Biology, University of North Carolina at Chapel Hill, Chapel Hill, NC 27599, United States of America

[d]Lineberger Comprehensive Cancer Center, University of North Carolina, 120 Mason Farm Road, Chapel Hill, NC 27599, United States of America

Abstract

Here we utilized the chromatin *in vivo* assay (CiA) mouse platform to directly examine the epigenetic barriers impeding the activation of the *CiA:Oct4* allele in mouse embryonic fibroblasts (MEF)s when stimulated with a transcription factor. The *CiA:Oct4* allele contains an engineered EGFP reporter replacing one copy of the *Oct4* gene, with an upstream Gal4 array in the promoter that allows recruitment of chromatin modifying machinery. We stimulated gene activation of the *CiA:Oct4* allele by binding a transcriptional activator to the Gal4 array. As with cellular reprograming, this process is inefficient with only a small percentage of the cells re-activating *CiA:Oct4* after weeks. Epigenetic barriers to gene activation potentially come from heavy DNA methylation, histone deacetylation, chromatin compaction, and other posttranslational marks (PTM) at the differentiated *CiA:Oct4* allele in MEFs. Using this platform, we performed a high-throughput chemical screen for compounds that increased the efficiency of activation. We found that Azacytidine and newer generation histone deacetylase (HDAC) inhibitors were the most efficient at facilitating directed transcriptional activation of this allele. We found one hit form

*Corresponding author at: The UNC Eshelman School of Pharmacy, Division of Chemical Biology and Medicinal Chemistry, 3209 Marsico Hall, 125 Mason Farm Road, Chapel Hill, NC 27599, United States of America., hathaway@unc.edu (N.A. Hathaway).

Author contributions

K.M.H.: Experimental design, collection of data, analysis of data, interpretation of data, and manuscript writing. K.M.K. and J.E.P.: experimental design and analysis for single-cell analysis experiments in Fig. 6 and Fig. S5, and manuscript writing. A.A.: Experimental design of Fig. 6, Fig. S7, and Fig. S8, and manuscript writing, E.Z.L: Experimental design, collection of data, analysis of data, and interpretation of data for Fig. S7; N.A.H.: Experimental design, analysis of data, interpretation of data, manuscript writing, and final approval of the manuscript.

Disclosure of potential conflicts of interest

The authors indicated no potential conflicts of interest.

Appendix A. Supplementary data

Supplementary data to this article can be found online at https://doi.org/10.1016/j.scr.2019.101470.

our screen, Mocetinostat, improved iPSC generation under transcription factor reprogramming conditions. These results separate individual allele activation from whole cell reprograming and give new insights that will advance tissue engineering.

Keywords

Epigenetics; Pharmacology; HDAC inhibitor; DNMT inhibitor; Chemical screen

1. Introduction

Regenerative medicine aims to replace damaged tissues with healthy engineered tissues (Tian et al., 2012; Walia et al., 2012). Many current regenerative medicine techniques use human derived stem cells (hESCs) from a donor to regenerate damaged tissues upon stem cell injection or to regenerate tissues *in vitro* which can be transplanted into the patient (Bongso and Richards, 2004; Mao and Mooney, 2015; Olson et al., 2011). Induced pluripotent stem cell (iPSC) therapies are a promising alternative within the regenerative medicine field allowing for individual treatments using iPSCs derived from a patient's own somatic cells (Kastenberg and Odorico, 2008; Mao and Mooney, 2015). The iPSC method avoids any potential ethical ramifications and has the advantage of treating patients with their own tissues. Furthermore, iPSCs specific tests can be done *in vitro* to personalize treatments (Bongso and Richards, 2004; Li and Li, 2014). Yet, a major barrier to application of iPSCs in clinical practice is that current iPSCs generated using the transcription factor induced reprogramming methods are inefficient and sometimes carcinogenic (Li et al., 2011; Medvedev et al., 2010; Takahashi and Yamanaka, 2006). Recent regenerative medicine research has found methods to efficiently generate safer iPSCs (Attwood and Edel, 2019; Cyranoski, 2018; Feng et al., 2009; Li and Li, 2014; Sanal, 2014; Sharma, 2016). Some of these techniques include small molecule facilitation of induced reprogramming which have resulted in more efficient cellular reprograming (Feng et al., 2009; Ichida et al., 2009; Li et al., 2011; Nie et al., 2012; Shi et al., 2008; Yuan et al., 2011; Zhu et al., 2010).

Previous studies have identified small molecules capable of increasing the efficiency of iPSC generation with transcription factor driven reprogramming methods. There has also been success in using small molecules to replace some transcription factors. However, finding an efficient small molecule cocktail that can alone efficiently activate reprogramming has been challenging (Li et al., 2009; Nie et al., 2012; Shi et al., 2008; Yuan et al., 2011; Zhou and Ding, 2010; Zhu et al., 2010). Klf4, c-Myc, *Oct4*, and Sox2 are typically employed in reprograming, these transcription factors irreversibly affect hundreds of genes. We wanted to examine epigenetic barriers to activation of a key pluripotency factor, *Oct4*. In this study, we performed a screen to identify small molecules that facilitate single allele activation in combination with a single transcriptional activator docked at the chromatin *in vivo* assay at *Oct4* (*CiA:Oct4*) allele. For this study, we chose to utilize a simian virus 40 large T antigen (SVT) infected cell line to immortalize our cells. This method made cells easier to array for a high throughput screen without having to worry about cell density or senescence. Notably, SVT immortalized cells have effectively been used by multiple groups to in regenerative medicine models (Kellermann et al., 1990; Kellermann et al., 1987; Poliard et al., 1995).

Oct4 expression is highly correlated with iPSC generation and is a key phenotypic indicator of successful iPSC generation (Hathaway et al., 2012; Ichida et al., 2009; Lin and Wu, 2015; Radzisheuskaya and Silva, 2014; Shi and Jin, 2010; Shimozaki et al., 2003; Zeineddine et al., 2014). The *Oct4* protein, encoded by the *POU5f1* (POU domain, class 5, transcription factor locus and belonging to the POU (Pit, Oct, Unc)) family, is described as a master pluripotency factor (Zeineddine et al., 2014). *Oct4* expression acts as a gatekeeper, driving molecular signaling cascades which maintain pluripotency in stem cells. *Oct4* is rapidly repressed as cells differentiate during mammalian development (Radzisheuskaya and Silva, 2014; Zeineddine et al., 2014). Hence, *Oct4* is a highly regulated genetic locus. The *Oct4* locus contains a distal enhancer, proximal enhancer, and proximal promoter which are regulated tightly throughout development (Kellner and Kikyo, 2010). Many different factors bind and regulate this locus. Notably, Dnmt3a and Dnmt3b methylate DNA at all three regulatory regions around the *Oct4* locus and promote silencing of the gene. Additionally, *Oct4* can form complexes with Nanog and HDAC2 resulting in silencing of the *Oct4* locus (Liang et al., 2008). High DNA methylation and low histone acetylation are present in somatic cells where *Oct4* has been completely silenced (Kellner and Kikyo, 2010). Fittingly, Azacytidine (DNA methyl transferase inhibitor (DNMTi)), Suberoylanilide Hydroxamic Acid (SAHA) (histone deacetylase inhibitor (HDACi)), and Valproic Acid (VPA) (HDACi) were among the first identified epigenetically relevant small molecules capable of increasing *Oct4* activation during transcription factor induced reprogramming (Feng et al., 2009; Huangfu et al., 2008). Other more recently discovered small molecules, such as *Oct4*-activating compound 1 (Li et al., 2012), BIX-01294 (Shi et al., 2008), RG108 (Shi et al., 2008), Sodium butyrate (Mali et al., 2010), AM580 (Wang et al., 2011), Tranylcypromine (Li et al., 2009), and DZNep (Hou et al., 2013) increase iPSC generation (Huangfu et al., 2008; Ichida et al., 2009; Nie et al., 2012) and also activate *Oct4* expression during transcription factor induced reprogramming methods. Among these identified small molecules, VPA was considered to be an effective *Oct4* activator under transcription factor induced reprogramming methods, providing a substantial increase in iPSC colony production (Feng et al., 2009).

We have developed a screening strategy using the CiA system in mouse embryonic fibroblast (MEF) cells. The CiA platform is a murine cell line with one *Oct4* allele replaced with an enhanced green fluorescent protein (EGFP) preceded by a Gal4 binding domain to which chromatin modifying machinery can be recruited through direct protein fusions to GAL4 or chemically induced proximity. The other *Oct4* allele in *CiA:Oct4* cells is wild type. From *CiA:Oct4* mice we generated MEF cell lines. We tested access to transcriptional machinery by recruiting a VP16 transcriptional activator to the *CiA:Oct4* locus as a GAL4 fusion protein, and observed a small amount of *CiA:Oct4* activation (~3% at the timepoint screened) as measured by GFP expression. We then performed a screen with a library of 959 small molecules to identify compounds that enhanced the ability of the tethered transcription factor to activate the *CiA:Oct4* locus. We validated the top small molecule activators from this screen with dose response analysis and compared it to previously described iPSC enhancers VPA, SAHA, and TSA. We found that small molecules identified by our screen outperformed VPA, SAHA, and TSA in single allele *Oct4* gene activation with VP16 recruitment. We then performed single-cell analysis of chosen successful *Oct4* activators

for 60 h following small molecule addition from small molecules DNMTi: Azacytidine and HDACis: Mocetinostat and Entinostat. From this experiment, we found that on a single-cell level, cells spontaneously turn on *CiA:Oct4* resulting in GFP expression that is passed on to daughter cells. Finally, we tested Mocetinostat with traditional four factor reprogramming and found this compound increased iPSC generation efficiency.

2. Results

2.1. Small molecule screen for facilitators of CiA:Oct4 activation

To identify small molecules targeting epigenetic pathways which restrict efficient activation of the *CiA:Oct4* locus, a high-throughput small molecule screen was performed (Fig. 1). We used an in-house curated set of small molecules with an epigenetic-targeted compound library (EpiG library), which contained a set of 959 small molecules. Some molecules are well characterized with known targets, others are derivatives from molecules that contain scaffolds similar to epigenetic inhibitors. This screen was performed with recruitment of the transcriptional activator VP16 or with a Gal4-DNA binding protein alone as a control.

Cells were infected with a Gal4-VP16 lentivirus and selected with puromycin. Compounds were added at 10 μM to cells on Day 0 and gene activation was measured by high-throughput flow cytometry after four days of compound treatment. (Fig. 1A). As a counter screen we used a lentiviral infection of a Gal4 protein alone without any transcriptional activation component (Fig. S1A). Flow cytometry readings for both screens were gated as indicated (Fig. S1B). Compounds were considered “hits” when > 5% of cells activated GFP. Compounds with high background fluorescence in the Gal4 counter screen were removed. The top 23 small molecule activators were rescreened for validation with a sequential dose curve treatment with concentrations ranging from 10 μM to 0.3 μM (Fig. S2A). Flow cytometry gating was performed as indicated (Fig. S2B). Based on dose response data, five small molecules were chosen for further analysis for activation of the *CiA:Oct4* locus including: Mocetinostat, Droxinostat, Entinostat, Tacedinaline, and Azacytidine. Azacytidine is a known potent DNMTi previously identified for increasing *Oct4* activation during transcription factor reprogramming conditions. Intriguingly, Mocetinostat Tacedineline and Entinostat all target HDAC −1, −2, and − 3 (Supplemental Table 1). The identification of HDAC inhibitors and DNMTi *Oct4* activators reinforced the importance of histone acetylation and DNA methylation on maintenance of chromatin state at the *Oct4* locus. It is important to note that although this study exclusively monitors *Oct4* expression, the four small molecules detailed in this study have widespread transcriptional perturbations which have been extensively documented in literature (Bijangi-Vishehsaraei et al., 2010; Cai et al., 2015; Delcuve et al., 2013; Fournel et al., 2008; Haberland et al., 2009; Lauffer et al., 2013; Liu et al., 2016; Loprevite et al., 2005; LoRusso et al., 1996; McCourt et al., 2012; Moradei et al., 2007; Píškala et al., 1981; Rosato et al., 2003; Saito et al., 1999; Wood et al., 2010; Yu et al., 2015). It is also possible that the facilitation of *Oct4* activation examined results from indirect effects of these inhibitors.

2.2. Validation of lead molecules

Hit compounds were validated and optimal compound concentration for gene activation was examined by a second round of dose response test on *CiA:Oct4* MEF cells (Fig. 2). To track the amount of gene activation and gain knowledge of cell transduction rates, *CiA:Oct4* MEF cells were infected with a lentiviral construct containing a Histone H2B monoCherry (H2B-mCh) tracer with a self-cleaving P2A peptide separating a Gal4-VP16. GFP and mCh were visualized using flow cytometry four days after small molecule treatment (Fig. 1A). Cells were fluorescence gated and the mCh positive cells were evaluated for GFP level as indicated (Fig. S3). Since only mCh cells are considered in this analysis the activation rates are higher as cells with lower transduction expression are excluded. For comparison, the Gal4-H2B-mCh-VP16 infected cells showed an average activation of 12% with a standard deviation of 2.8. Mocetinostat demonstrated 29% *CiA:Oct4* activation at 0.625 μM. Tacedinaline demonstrated 20% *CiA:Oct4* activation at 10 μM. Entinostat demonstrated 32% *CiA:Oct4* activation at 0.312 μM. Azacytidine demonstrated the most effective activation at 5 μM (57%), but 2.5 μM treated cells had better cell morphology by microscope analysis and still had 45% activation. Droxinostat did not demonstrate significant activation following rescreening and was removed from further study.

Interestingly, four of the five small molecules (Mocetinostat, Tacedinaline, Entinostat, and Azacytidine) identified by this screen were more effective than VPA, SAHA, and TSA in single allele *CiA:Oct4* activation. In this assay, the activation in the presence of VPA treatment was not significant. This could be due to moderate cell death we observed in the presence of VPA (data not shown). Likewise, SAHA demonstrated no significant activation while TSA allowed for mild increased activation at a dose of 0.08 μM (16% *CiA:Oct4* activation). It should be noted that the time frame of our analysis was much shorter than the time frame of whole cell reprograming, and the barriers of single allele activation may be different than network activation by transcription factor cocktails.

2.3. Temporal analysis of chemical facilitated CiA:Oct4 activation

To understand the dynamics of small molecule facilitated gene activation by a directed transcription factor in a population of cells, gene activation was monitored by time lapse microscopy and flow cytometry over 70 h following small molecule treatment as indicated (Fig. 3A). Digital analysis of images was used to identify total cell population in a frame of view and then to count GFP positive cells (Fig. S4). This approach of monitoring gene activation in live cells allowed us to identify key transformation points in allele activation. We found that Entinostat and Mocetinostat accelerated transcription factor driven gene activation, with activation peaks detected by 30 h (Fig. 3B). Azacytidine showed slower gene activation from hours 0–30, while rapid gene activation from hours 30–60 and peak activation at hour 70. These results suggested that HDAC inhibition results the facilitation of early *CiA:Oct4* activation; however, at later time points some effects are lost. Comparably, Azacytidine resulted in slow and constant triggered activation in conjunction with tethered transcriptional machinery. To further understand the durability of small molecule effects on activation of the *Oct4* locus by transcription activator docking, cells were treated with compound for four days then released for four days by washout of small molecule (Fig. 4A). We found cells with higher transcriptional activator driven expression from HDACi

treatment rapidly lost gene activation after four days of HDACi washout. Comparatively, cells treated with Azacytidine and directed transcriptional activator maintained higher levels gene activation even after four days of small molecule release (Fig. 4B).

2.4. Single cell analysis of chemical facilitated CiA:Oct4 activation

To study *CiA:Oct4* activation response on a single-cell level to transcriptional activator tethering in conjunction with HDACi and DNMTi treatment, cells were tracked through the H2B-mCh tracer and single-cell nuclear GFP intensity was quantified at each time point. We found that *CiA:Oct4* nuclear GFP average mean intensity increased at different rates in individual cells tracked. However, there was a clear difference in the stimulated activation between control cells and small molecule treated cells. Untreated control cells had gradual expression changes in general while small molecule treated samples demonstrated spontaneous rapid allele activation. A common theme throughout both control and small molecule treated cells was that daughter cells tended to maintain parental expression patterns after cell divisions. Namely, cells that were GFP negative tended to stay GFP negative and cells that were GFP positive tended to have progeny that were also GFP positive (Fig. 5). These findings are consistent with the model where *Oct4* expression is driven by the expression of the *Oct4* alleles passed down from parental cells (Wolff et al., 2018). As a control, the expression of GFP compared to nuclear mCh expression was also tracked (Fig. S5). In conclusion, these results lead us to believe treatment with Mocetinostat and/or Azacytidine are the most effective compounds among those tested to facilitate *Oct4* activation by transcriptional activators.

2.5. Small molecule effects on cell cycle and viability

To understand the effect of small molecules on cell cycle we used a standard propidium iodide staining assay to measure total DNA content per cell. To understand and effects on cell viability we performed an alamarBlue assay which measures metabolically active live cells. We treated cells for five days with small molecule as indicated (Fig. S6A). On the fourth day all cell wells were split to ensure logarithmic growth at our assay point. On the fifth day, both cell viability and cell cycle analyses were conducted. It was found that cell viability was not changed in Mocetinostat, Entinostat, and Tacedinealine at optimal treatment concentrations from our dose response analysis, while Azacytidine and VPA standard treatment resulted in measurable cell cytotoxicity (Fig. S6B). We did not determine any large perturbations to the cell cycle upon propidium iodide staining (Fig. S6C, Gated in Fig. S6D).

2.6. Mocetinostat increases CiA:Oct4 activation during transcription factor reprogramming

As a final test to see if molecules identified by our single allele activation method could help advance cell reprograming techniques, we compared Mocetinostat identified here with Azacytidine and generated iPSC by 4-factor reprograming. We infected *CiA:Oct4* MEFs with a polycistronic vector containing *Oct4*, Sox2, Klf, and cMyc separated by self-cleaving peptides with a tetracycline inducible promoter system (Carey et al., 2009). (Fig. 6A). We found that Mocetinostat increased activation of *Oct4*-GFP, a phenotypic indicator of cell reprogramming to 22% GFP+ (Fig. 6B, Gated in Fig. S7D–E). The control

(Doxycycline treated cells without small molecule addition) demonstrated a lower level of GFP expression. Notably, the addition of small molecules to all polycistronic vector infected cells resulted in small activation potentially from small molecules facilitation in overcoming doxycycline control of the four-factor cassette (Fig. S7C). We confirmed successful iPSC colony generation through alkaline phosphatase staining and morphological changes which resembled iPSC colonies (Fig. S7A–B, Fig. S8).

3. Discussion

We determined from this small molecule screen and follow-up studies that four compounds (Mocetinostat, Tacedinaline, Entinostat, and Azacytidine) demonstrated robust and reproducible single *CiA:Oct4* allele activation when used in conjunction with transcriptional activator recruitment. In ideal conditions, Azacytidine demonstrated a ~60% *CiA:Oct4* activation, which is the highest change in *Oct4*-GFP expression recorded in a population of cells due to a single transcription factor and small molecule combination acting on *Oct4*. Interestingly, of the top five small molecule activators from the original screen, four were HDAC inhibitors and the top hit is a previously described *Oct4* activator and DNA methylation inhibitor, Azacytidine (Huangfu et al., 2008). This reinforces previous findings that DNA methylation and histone acetylation play major roles in determining *Oct4* expression levels. But also adds new classes of HDAC inhibitors that should be further examined in iPSC generation work. Notably, Mocetinostat, Tacedinaline, Entinostat, and Azacytidine outperformed TSA, SAHA, and VPA suggesting that single allele activation may not have the same requirements as whole cell network transcription factor reprogramming conditions.

We were able to further reveal gene activation dynamics through our small molecule treatment and release study (Fig. 4B). We found that HDACi resulted in rapid gene activation which was rapidly lost upon small molecule release. Comparatively, DNMTi resulted in slower gene activation which was maintained even after the small molecule was removed from the system. We believe HDAC inhibition resulted in rapid reversible gene activation while DNMTi resulted in slow and more static gene activation. Previous studies have supported the idea that loss of histone acetylation results in reversible epigenetic memory, while DNA methylation accumulation results in irreversible epigenetic memory (Bintu et al., 2016). Our study demonstrates that the other side of the model is true as well; it supports a model through which histone acetylation accumulation results in rapid and reversible gene activation, while DNA de-methylation results in irreversible gene activation. Finally, we demonstrated that one small molecule identified by this screen, Mocetinostat, lead to a 22% of *CiA:Oct4* activation at an early timepoint in iPSC generation. Our work indicates that Mocetinostat could be a strong candidate for future small molecule facilitated iPSC generation studies.

4. Conclusion

In conclusion, we identified the following small molecules: Azacytidine, Mocetinostat, Tacedinaline, and Entinostat which stimulated high single allele *Oct4* activation when combined with the directed recruitment of transcriptional machinery. Our results provide for

a robust epigenetic screen for endogenous single allele *Oct4* activation chemical enhancers combining a directed transcription factor and small molecule. Additionally, we demonstrated dynamics of *Oct4* single allele activation through treatment using HDACi or DNMTi pathways. We found that HDAC inhibition seemed to result in primary peak activation occurring by 30 h while DNMT inhibition resulted in gradual activation with peak activation by hour 60. Interestingly, DNMT inhibition resulted in activation that was sustained even after four days release of small molecules, while HDAC inhibition resulted in activation that was almost completely lost after four days. This demonstrated models of epigenetic memory where histone acetylation levels are more dynamic than DNA methylation levels and can result in corresponding more dynamic activation with histone acetylation accumulation compared to slower DNA methylation loss. We further found exploration of *CiA:Oct4* MEFs expression on a single-cell level revealed that *Oct4* activation was spontaneous throughout the experiment and active *CiA:Oct4* expression state can be stably passed through cellular generations. Finally, we found that the small molecule Mocetinostat identified in this study was successful in increasing iPSC generation.

5. Methods

5.1. Generation of CiA:Oct4 SVT-MEFs

CiA:Oct4 MEF cell lines immortalized by infection of simian virus 40 large T antigen, were obtained and cultured as previously described (Hathaway et al., 2012). Briefly, cells were cultured at 37 °C 5% CO_2 conditions. Base media was either FluoroBrite DMEM Media (ThermoFisher, A1896701) for imaging, or DMEM (Corning, MT10013CV) for standard cell culture. Media was supplemented with 10% FBS (Gibco, Lot:1972526), 10 mM HEPES pH 7.5, 10 mM NEAA, 0.1% 1000 × 2-betamercaptoethanol (Gibco, 21,985,023), 1% 100× Penn-Strep (Corning, 30–002-CI). Additionally, L-Glutamine (Corning, 25005CI) at 4 mM was added to FluoroBrite media.

5.2. Description of plasmids

nLV-EF-1a-Gal4-VP16-PGK-Puro (N114, Addgene, Plasmid #44014) and nLV-EF-1a-Gal4-Stop-PGK-Puro (N113, Addgene, Plasmid #44176) were previously described.

nLV-EFn-1a-Gal4-VP16-P2A-H2B-mCh-PGK-Puro (K114mC) was developed by a PCR stitching Gal4-VP16-P2A P2A-H2B-mCh and in fusion cloning the product into a NotI linearized nLV-Dual Promoter EF-1a-MCS-PGK-Puro (N103) using In-fusion HD cloning kit (Clontech). Plasmid and plasmid map are available on Addgene: TetO-FUW-OKSIM (Addgene, Plasmid #20321) and FUW-M2rtTA (Addgene, Plasmid # 20342).

5.3. Lentiviral infection of CiA:Oct4 SVT-MEFs

15 million 293 T lentiX cells (Clontech) were co-transfected with gene delivery vector (N114, K114mC, or N113) and packaging vectors pspax2 (Addgene, Plasmid #12260) and pMD2.G (Addgene, Plasmid # 12259) with PEI (Polysciences Inc., 24,765) and cultured for 48 h to produce lentivirus. Lentivirus was pelleted via ultracentrifugation with a Beckman SW32Ti rotor a ~72,000 xg and resuspended in 150uL PBS. 60,000 *CiA:Oct4* MEFs

were infected with 30uL of concentrated lentivirus. Puromycin selection of MEF cells was performed at a concentration of 2.5 μg/ml.

5.4. Small molecule screen

EpiG set of three 384-well compound plates was used in assay, compounds were screened at 10 μM. *CiA:Oct4* MEFs were cultured in standard conditions then infected with lentivirus (N114, N113) and treated with small molecules for four days at 10 μM. Screens were performed in three separate screens. Cells were analyzed by Flow Cytometry on the iQue or iQue Screener Plus. Analysis gating was performed using FlowJo as indicated (Fig. S1B).

5.5. Dose-response of small molecule treatment

CiA:Oct4 MEFs were cultured in standard conditions then infected with lentivirus (N114, N113, K114mC) and treated with small molecules for four days in a dose dependent manner and then released from small molecule treatment for four days. The small molecule treatment on the *CiA:Oct4* MEFs were dosed as follows: Droxinostat (10 μM, 5 μM, 2.5 μM. 1.25 μM, 0.625 μM, 0.312 μM**, 0.156 μM, 0.078 μM, 0.039 μM, 0.019 μM, 0.010 μM, 0.005 μM). Mocetinostat (1.25 μM, 0.625 μM, 0.3125 μM, 0.1256 μM. 0.08 μM, 0.04 μM**, 0.20 μM, 0.01 μM, 0.005 μM, 0.002 μM, 0.001 μM, 0.0006 μM), Tacedinaline (10 μM, 5 μM, 2.5 μM. 1.25 μM, 0.625 μM, 0.312 μM**, 0.156 μM, 0.078 μM, 0.039 μM, 0.019 μM, 0.010 μM, 0.005 μM) Entinostat (2.5 μM, 1.25 μM, 0.625 μM, 0.3125 μM, 0.1256 μM, 0.08 μM**, 0.04 μM, 0.02 μM, 0.01 μM, 0.005 μM, 0.002 μM, 0.001 μM), Azacytidine (10 μM, 5 μM, 2.5 μM. 1.25 μM, 0.625 μM, 0.312 μM**, 0.156 μM, 0.078 μM, 0.039 μM, 0.019 μM,0.010 μM, 0.005 μM), TSA (0.16 μM, 0.08 μM, 0.04 μM, 0.02 μM, 0.01 μM, 0.005 μM**, 0.0025 μM, 0.0013 μM, 0.0006 μM, 0.0003 μM, 0.0002 μM, 0.0002 μM) VPA (5000 μM, 2500 μM, 1250 μM, 625 μM, 312.5 μM, 156.25 μM**, 78.12 μM, 39.06 μM, 19.5 μM, 9.7 μM, 4.8 μM, 2.4 μM) SAHA (10 μM, 5 μM, 2.5 μM. 1.25 μM, 0.625 μM, 0.312 μM**, 0.156 μM, 0.078 μM, 0.039 μM, 0.019 μM, 0.010 μM, 0.005 μM). ($n \geq 3$ except at indicated ** where $n = 2$) Cells were imaged by the IN Cell Analyzer 2200 on Day 4 and Day 8 following lentiviral infection. Cells were analyzed by Flow Cytometry on the iQue Screener Plus. Analysis gating was performed using FlowJo as indicated (Fig. S3).

5.6. Small molecule time lapse imaging

CiA:Oct4 MEFs were cultured in standard conditions then infected with lentivirus (N114, N113, K114mC) and treated with small molecules for four days in a dose dependent manner. The small molecule treatment dosage was follows: Droxinostat (10 μM, 5 μM, 2.5 μM. 1.25 μM, 0.625 μM, 0.312 μM, 0.156 μM, 0.078 μM, 0.039 μM, 0.019 μM, and 0.010 μM) Mocetinostat (5 μM, 2.5 μM. 1.25 μM, 0.625 μM, 0.312 μM, 0.156 μM, 0.078 μM, 0.039 μM, 0.019 μM, 0.010 μM, and 0.005 μM), Tacedinaline (5 μM, 2.5 μM. 1.25 μM, 0.625 μM, 0.312 μM, 0.156 μM, 0.078 μM, 0.039 μM, 0.019 μM, 0.010 μM, and 0.005 μM), Entinostat (5 μM, 2.5 μM. 1.25 μM, 0.625 μM, 0.312 μM, 0.156 μM, 0.078 μM, 0.039 μM, 0.019 μM, 0.010 μM, and 0.005 μM). *CiA:Oct4* SVT-MEFs were imaged every two hours after 24 h (for 14 h) and after 48 h (for 14 h) by the GE IN Cell Analyzer, as well as once every 24 h.

5.7. Single-cell analysis

CiA:Oct4 MEFs were cultured in standard conditions and treated with small molecules for four days in a dose dependent manner. The small molecule treatment dosage was follows: 2.5 μM for Azacytidine, 630 nM Entinostat and 80 nM Mocetinostat. *CiA:Oct4* SVT-MEFs were imaged every 35 min from hours 0 to 60 by the GE IN Cell Analyzer. Scale bar in videos is 50um. (Supplemental Videos) Cells were segmented, tracked and annotated in a semi-automatic way as described previously (Borland et al., 2018) using a set of scripts developed in Fiji (Schindelin et al., 2012). GFP (*Oct4*) and H2B-mCherry signals were calculated as a mean value of pixels within defined nuclear regions. Family trees were rendered using EteToolkit library (Huerta-Cepas et al., 2016) in Python 4.5.4 Anaconda (Anaconda, 2016). Cell death rate was calculated as a ratio of tracks ending in cell death to all possible track endings, namely: end of the experiment, cell leaving a field of view, mitosis or cell death.

5.8. Microscope image acquisition

IN Cell Analyzer 2200: Chip type front illuminated sCMOS, Chip size 2560 × 2160 pixels. Pixel size 6.5 μm. Readout speeds 95 MHz, 286Mhz, Readout modes Rolling shutter, global shutter. Camera interface Camera-link. Bit depth 15 bit. Quantum efficiency ~60% dynamic range 1:15,000. Read noise 1.5 e at 33 fps 2e at 100fps. Magnification (20× objective) IN Cell Analyzer 2200 software for acquisition and IN Cell Developer for image processing. Pictures of cells were taken at 37 degrees Celsius in FluoroBrite media. Images were taken with the FITC 525, Brightfield, and Cy3 filters. Images were taken in 2-D imaging setting.

6. Cell viability/proliferation

CiA:Oct4 MEFs were cultured in standard conditions and treated with small molecules for five days in a dose dependent manner as indicated (Fig. S6A). High, Medium, and Low treatment conditions are as follows:. Mocetinostat (High = 1.6 μM, Medium = 0.16 μM, Low = 0.05 μM, $n = 8$), Tacedinaline (High = 30 μM, Medium = 10 μM, Low = 3.3 μM, $n = 8$), Entinostat (High = 12.5 μM, Medium = 1.25 μM, Low = 0.42 μM, $n = 8$), DMSO ($n = 28$), Azacytidine (High = 25 μM, Medium = 2.5 μM, Low = 0.8 μM, $n = 8$), VPA (High = 6000 μM, Medium = 2000 μM, Low = 667 μM, $n = 8$)). Cells were split on day four to 10,000 cells/ml. alamarBlue reagent (Cat # DAL1025) was added on Day 5 to 10% of well volume with standard conditions and incubated for 16 h before visualization on the GloMax Discover Serial Number 9700000261 and Software Version 3.0.0.

6.1. Cell cycle analysis

CiA:Oct4 MEFs were cultured in standard conditions and treated with small molecules for five days in a dose dependent manner as indicated in (Fig. S6A). Treatment conditions are as follows: Mocetinostat (0.16 μM, $n = 3$), Tacedinaline (10 μM, $n = 3$), Entinostat (1.25 μM, $n = 3$), DMSO ($n = 3$), Azacytidine (2.5 μM, $n = 3$), VPA (2000 μM, $n = 3$)). To stain for cell cycle phases, a propidium iodide assay was performed after ethanol fixation. Cells were analyzed by flow cytometry on an iQue Screener Plus. Gating of cells was performed as indicated (Fig. S6D).

6.2. Induction of pluripotent stem cells with small molecule treatment

CiA:Oct4 SVT-MEF cells were infected with TetO-FUW-OKSIM and FUW-M2rtTA on Day −15 as indicated in Fig. 6A. On Day 0, cells were treated with either DMSO (Control), 2.5 μM Azacytidine, or 156 nM Mocetinostat accompanied with (Fig. 6B) or without Doxycycline (Fig. S7C). Flow cytometry was performed on Day 4. Cells cultured for longer than four days were treated with small molecules alternating on and off every 2–3 days. Gating strategy is demonstrated in Fig. S7C. Imaging of cells for Fig. 6A was performed on Day 4. (Fig. S7A). Alkaline phosphatase staining was performed with Reprocell Alkaline Phosphate Staining Kit (Cat # NC0088922). Alkaline phosphatase staining was performed at various times ranging from 20 to 60 days after infection as indicated in figures.

Supplementary Material

Refer to Web version on PubMed Central for supplementary material.

Acknowledgements

We would like to thank the members of the Hathaway lab and the Center for Integrative Chemical Biology and Drug Discovery for helpful advice and technical assistance, especially S. Frye, K. Pearce, L. James, and B. Hardy. We thank P. Vignaux for critical reading of the manuscript. The authors thank B. Price for data visualization with Python Programming. We thank the Flow Cytometry Core University of North Carolina funded by P30 CA016086 Cancer Center Core Support Grant to the UNC Lineberger Comprehensive Cancer Center. We also thank S. Coquery and J. Dow for technical assistance with flow cytometry. This work was in part supported by grants from the U.S. National Institutes of Health, Grant R01GM118653 (to N.A.H.) and Grant DP2-HD091800-01 (to J.E.P.). K.M.H was supported National Science Foundation Grant No. DGE-1650116 and by a training grant from NIGMS under award T32 GM119999. This material is based upon work supported by the National Science Foundation Graduate Research Fellowship Program. Any opinions, findings, and conclusions or recommendations expressed in this material are those of the author(s) and do not necessarily reflect the views of the National Science Foundation.

References

Anaconda, 2016. Anaconda Software Distribution. Comput. Softw

Attwood SW, Edel MJ, 2019. iPS-cell technology and the problem of genetic instability-can it ever be safe for clinical use? J. Clin. Med 8, 288. 10.3390/jcm8030288.

Bijangi-Vishehsaraei K, Huang S, Safa AR, Saadatzadeh MR, Murphy MP, 2010. 4-(4-Chloro-2-methylphenoxy)-N-hydroxybutanamide (CMH) targets mRNA of the c-FLIP variants and induces apoptosis in MCF-7 human breast cancer cells. Mol. Cell. Biochem 342, 133–142. 10.1007/s11010-010-0477-7. [PubMed: 20446019]

Bintu L, Yong J, Antebi YE, McCue K, Kazuki Y, Uno N, Oshimura M, Elowitz MB, 2016. Dynamics of epigenetic regulation at the single-cell level. Science 351, 720–724. 10.1126/science.aab2956. [PubMed: 26912859]

Bongso A, Richards M, 2004. History and perspective of stem cell research. Best Pract. Res. Clin. Obstet. Gynaecol 18, 827–842. 10.1016/j.bpobgyn.2004.09.002. [PubMed: 15582541]

Borland D, Yi H, Grant GD, Kedziora KM, Chao HX, Haggerty RA, Kumar J, Wolff SC, Cook JG, Purvis JE, 2018. The cell cycle browser: an interactive tool for visualizing, simulating, and perturbing cell-cycle progression. Cell Syst 7, 180–184.e4. 10.1016/j.cels.2018.06.004. [PubMed: 30077635]

Cai J, Zhang Q, Lin K, Hu L, Zheng Y, 2015. The effect of MGCD0103 on CYP450 isoforms activity of rats by cocktail method. Biomed. Res. Int 2015, 517295. 10.1155/2015/517295. [PubMed: 26357656]

Carey BW, Markoulaki S, Hanna J, Saha K, Gao Q, Mitalipova M, Jaenisch R, 2009. Reprogramming of murine and human somatic cells using a single polycistronic vector. Proc. Natl. Acad. Sci 106, 157–162. 10.1073/pnas.0811426106. [PubMed: 19109433]

Cyranoski D, 2018. Reprogrammed' stem cells to be tested in people with Parkinson's disease. Nature. 10.1038/d41586-018-07407-9.

Delcuve GP, Khan DH, Davie JR, 2013. Roles of histone deacetylases in epigenetic regulation: Emerging paradigms from studies with inhibitors. In: Epigenetics and Pathology: Exploring Connections between Genetic Mechanisms and Disease Expression. Apple Academic Press, pp. 143–171. 10.1201/b16304.

Feng B, Ng JH, Heng JCD, Ng HH, 2009. Molecules that promote or enhance reprogramming of somatic cells to induced pluripotent stem cells. Cell Stem Cell 4, 301–302. 10.1016/j.stem.2009.03.005. [PubMed: 19341620]

Fournel M, Bonfils C, Hou Y, Yan PT, Trachy-Bourget M-C, Kalita A, Liu J, Lu A-H, Zhou NZ, Robert M-F, Gillespie J, Wang JJ, Ste-Croix H, Rahil J, Lefebvre S, Moradei O, Delorme D, Macleod AR, Besterman JM, Li Z, 2008. MGCD0103, a novel isotype-selective histone deacetylase inhibitor, has broad spectrum antitumor activity in vitro and in vivo. Mol. Cancer Ther 7, 759–768. 10.1158/1535-7163.MCT-07-2026. [PubMed: 18413790]

Haberland M, Montgomery RL, Olson EN, 2009. The many roles of histone deacetylases in development and physiology: implications for disease and therapy. Nat. Rev. Genet (1), 32–42. 10.1038/nrg2485. [PubMed: 19065135]

Hathaway NA, Bell O, Hodges C, Miller EL, Neel DS, Crabtree GR, 2012. Dynamics and memory of heterochromatin in living cells. Cell 149, 1447–1460. [PubMed: 22704655]

Hou P, Li Y, Zhang X, Liu C, Guan J, Li H, Zhao T, Ye J, Yang W, Liu K, Ge J, Xu J, Zhang Q, Zhao Y, Deng H, 2013. Pluripotent stem cells induced from mouse somatic cells by small-molecule compounds. Science 341, 651–654. 10.1126/science.1239278. [PubMed: 23868920]

Huangfu D, Maehr R, Guo W, Eijkelenboom A, Snitow M, Chen AE, Melton D.a, 2008. Induction of pluripotent stem cells by defined factors is greatly improved by small-molecule compounds. Nat. Biotechnol 26, 795–797. [PubMed: 18568017]

Huerta-Cepas J, Serra F, Bork P, 2016. ETE 3: reconstruction, analysis, and visualization of Phylogenomic data. Mol. Biol. Evol 33, 1635–1638. 10.1093/molbev/msw046. [PubMed: 26921390]

Ichida JK, Blanchard J, Lam K, Son EY, Chung JE, Egli D, Loh KM, Carter AC, Di Giorgio FP, Koszka K, Huangfu D, Akutsu H, Liu DR, Rubin LL, Eggan K, 2009. A small-molecule inhibitor of Tgf-β signaling replaces Sox2 in reprogramming by inducing Nanog. Cell Stem Cell 5, 491–503. [PubMed: 19818703]

Kastenberg ZJ, Odorico JS, 2008. Alternative sources of pluripotency: science, ethics, and stem cells. Transplant. Rev 22, 215–222. 10.1016/j.trre.2008.04.002.

Kellermann O, Buc-Caron MH, Gaillard J, 1987. Immortalization of precursors of endodermal, neuroectodermal and mesodermal lineages, following the introduction of the simian virus (SV40) early region into F9 cells. Differentiation 35, 197–205. 10.1111/j.1432-0436.1987.tb00169.x. [PubMed: 2833421]

Kellermann O, Buc-Caron MH, Marie PJ, Lamblin D, Jacob F, 1990. An immortalized osteogenic cell line derived from mouse teratocarcinoma is able to mineralize in vivo and in vitro. J. Cell Biol 110, 123–132. 10.1083/jcb.110.1.123. [PubMed: 2153146]

Kellner S, Kikyo N, 2010. Transcriptional regulation of the Oct4 gene, a master gene for pluripotency. Histol. Histopathol 25, 405–412. [PubMed: 20054811]

Lauffer BEL, Mintzer R, Fong R, Mukund S, Tam C, Zilberleyb I, Flicke B, Ritscher A, Fedorowicz G, Vallero R, Ortwine DF, Gunzner J, Modrusan Z, Neumann L, Koth CM, Lupardus PJ, Kaminker JS, Heise CE, Steiner P, 2013. Histone Deacetylase (HDAC) inhibitor kinetic rate constants correlate with cellular histone acetylation but not transcription and cell viability. J. Biol. Chem 288, 26926–26943. 10.1074/jbc.M113.490706. [PubMed: 23897821]

Li S, Li Q, 2014. A promising approach to iPSC-based cell therapy for diabetic wound treatment: direct lineage reprogramming. Mol. Cell. Endocrinol 393, 8–15. 10.1016/j.mce.2014.05.025. [PubMed: 24911883]

Li W, Zhou H, Abujarour R, Zhu S, Joo JY, Lin T, Hao E, Schöler HR, Hayek A, Ding S, 2009. Generation of human-induced pluripotent stem cells in the absence of exogenous Sox2. Stem Cells 27, 2992–3000. 10.1002/stem.240. [PubMed: 19839055]

Li Y, Zhang Q, Yin X, Yang W, Du Y, Hou P, Ge J, Liu C, Zhang W, Zhang X, Wu Y, Li H, Liu K, Wu C, Song Z, Zhao Y, Shi Y, Deng H, 2011. Generation of iPSCs from mouse fibroblasts with a single gene, Oct4, and small molecules. Cell Res. 21, 196–204. 10.1038/cr.2010.142. [PubMed: 20956998]

Li W, Tian E, Chen Z-X, Sun G, Ye P, Yang S, Lu D, Xie J, Ho T-V, Tsark WM, Wang C, Horne DA, Riggs AD, Yip MLR, Shi Y, 2012. Identification of Oct4-activating compounds that enhance reprogramming efficiency. Proc. Natl. Acad. Sci 109, 20853–20858. 10.1073/pnas.1219181110. [PubMed: 23213213]

Liang J, Wan M, Zhang Y, Gu P, Xin H, Jung SY, Qin J, Wong J, Cooney AJ, Liu D, Songyang Z, 2008. Nanog and Oct4 associate with unique transcriptional repression complexes in embryonic stem cells. Nat. Cell Biol 10, 731–739. 10.1038/ncb1736. [PubMed: 18454139]

Lin T, Wu S, 2015. Reprogramming with small molecules instead of exogenous transcription factors. Stem Cells Int. 2015, 1–11. 10.1155/2015/794632.

Liu J, Li G, Wang X, Wang L, Zhao R, Wang J, Kong Y, Ding J, Li J, Zhang L, 2016. Droxinostat, a histone Deacetylase inhibitor, induces apoptosis in hepatocellular carcinoma cell lines via activation of the mitochondrial pathway and Downregulation of FLIP. Transl. Oncol 9, 70–78. 10.1016/j.tranon.2016.01.004. [PubMed: 26947884]

Loprevite M, Tiseo M, Grossi F, Scolaro T, Semino C, Pandolfi A, Favoni R, Ardizzoni A, 2005. In vitro study of CI-994, a histone deacetylase inhibitor, in non-small cell lung cancer cell lines. Oncol. Res 15, 39–48. [PubMed: 15839304]

LoRusso PM, Demchik L, Foster B, Knight J, Bissery MC, Polin LM, Leopold WR, Corbett TH, 1996. Preclinical antitumor activity of CI-994. Investig. New Drugs 14, 349–356. [PubMed: 9157069]

Mali P, Chou BK, Yen J, Ye Z, Zou J, Dowey S, Brodsky RA, Ohm JE, Yu W, Baylin SB, Yusa K, Bradley A, Meyers DJ, Mukherjee C, Cole PA, Cheng L, 2010. Butyrate greatly enhances derivation of human induced pluripotent stem cells by promoting epigenetic remodeling and the expression of pluripotency-associated genes. Stem Cells 28, 713–720. 10.1002/stem.402. [PubMed: 20201064]

Mao AS, Mooney DJ, 2015. Regenerative medicine: current therapies and future directions. Proc. Natl. Acad. Sci 112, 14452–14459. 10.1073/pnas.1508520112. [PubMed: 26598661]

McCourt C, Maxwell P, Mazzucchelli R, Montironi R, Scarpelli M, Salto-Tellez M, O'Sullivan JM, Longley DB, Waugh DJJ, 2012. Elevation of c-FLIP in castrate-resistant prostate cancer antagonizes therapeutic response to androgen receptor-targeted therapy. Clin. Cancer Res 18, 3822–3833. 10.1158/1078-0432.CCR-11-3277. [PubMed: 22623731]

Medvedev SP, Shevchenko AI, Zakian SM, 2010. Induced pluripotent stem cells: problems and advantages when applying them in regenerative medicine. Acta Nat. 2, 18–28.

Moradei OM, Mallais TC, Frechette S, Paquin I, Tessier PE, Leit SM, Fournel M, Bonfils C, Trachy-Bourget M-C, Liu J, Yan TP, Lu A-H, Rahil J, Wang J, Lefebvre S, Li Z, Vaisburg AF, Besterman JM, 2007. Novel aminophenyl benzamide-type histone deacetylase inhibitors with enhanced potency and selectivity. J. Med. Chem 50, 5543–5546. 10.1021/jm701079h. [PubMed: 17941625]

Nie B, Wang H, Laurent T, Ding S, 2012. Cellular reprogramming: a small molecule perspective. Curr. Opin. Cell Biol (6), 784–792. 10.1016/j.ceb.2012.08.010. [PubMed: 22959962]

Olson JL, Atala A, Yoo JJ, 2011. Tissue engineering: current strategies and future directions. Chonnam Med. J 47 (1). 10.4068/cmj.2011.47.1.1.

Píškala A, Hanna NB, Buděsínský M, Cihák A, Veselý J, 1981. Synthesis and biological activity of 2′-deoxy-6-methyl-5-azacytidine and its alpha-D-anomer. Nucleic Acids Symp. Ser 83–86. [PubMed: 6170945]

Poliard A, Nifuji A, Loric S, Lamblin D, Launay JM, Kellermann O, Kellermann O, 1995. Immortalization of committed precursor cells from mouse teratocarcinoma using an adenovirus-SV40 recombinant plasmid. Methods Cell Sci. 17, 103–109. 10.1007/BF00986658.

Radzisheuskaya A, Silva JCR, 2014. Do all roads lead to Oct4? The emerging concepts of induced pluripotency. Trends Cell Biol. (5), 275–284. [PubMed: 24370212]

Rosato RR, Almenara JA, Grant S, 2003. The histone deacetylase inhibitor MS-275 promotes differentiation or apoptosis in human leukemia cells through a process regulated by generation of

reactive oxygen species and induction of p21CIP1/WAF11. Cancer Res. 63, 3637–3645. [PubMed: 12839953]

Saito A, Yamashita T, Mariko Y, Nosaka Y, Tsuchiya K, Ando T, Suzuki T, Tsuruo T, Nakanishi O, 1999. A synthetic inhibitor of histone deacetylase, MS-27–275, with marked in vivo antitumor activity against human tumors. Proc. Natl. Acad. Sci. U. S. A 96, 4592–4597. [PubMed: 10200307]

Sanal MG, 2014. A highly efficient method for generation of therapeutic quality human pluripotent stem cells by using naive induced pluripotent stem cells nucleus for nuclear transfer. SAGE open Med 2, 2050312114550375. 10.1177/2050312114550375.

Schindelin J, Arganda-Carreras I, Frise E, Kaynig V, Longair M, Pietzsch T, Preibisch S, Rueden C, Saalfeld S, Schmid B, Tinevez JY, White DJ, Hartenstein V, Eliceiri K, Tomancak P, Cardona A, 2012. Fiji: an open-source platform for biological-image analysis. Nat. Methods 10.1038/nmeth.2019.

Sharma R, 2016. iPS cells—the triumphs and tribulations. Dent. J 4, 19. 10.3390/dj4020019.

Shi G, Jin Y, 2010. Role of Oct4 in maintaining and regaining stem cell pluripotency. Stem Cell Res Ther 1, 39. [PubMed: 21156086]

Shi Y, Desponts C, Do JT, Hahm HS, Schöler HR, Ding S, 2008. Induction of pluripotent stem cells from mouse embryonic fibroblasts by Oct4 and Klf4 with small-molecule compounds. Cell Stem Cell 3, 568–574. 10.1016/j.stem.2008.10.004. [PubMed: 18983970]

Shimozaki K, Nakashima K, Niwa H, Taga T, 2003. Involvement of Oct3/4 in the enhancement of neuronal differentiation of ES cells in neurogenesis-inducing cultures. Development 130, 2505–2512. [PubMed: 12702663]

Takahashi K, Yamanaka S, 2006. Induction of pluripotent stem cells from mouse embryonic and adult fibroblast cultures by defined factors. Cell 126, 663–676. 10.1016/j.cell.2006.07.024. [PubMed: 16904174]

Tian C, Ambroz RJ, Sun L, Wang Y, Ma K, Chen Q, Zhu B, Zheng JC, 2012. Direct conversion of dermal fibroblasts into neural progenitor cells by a novel cocktail of defined factors. Curr. Mol. Med 12, 126–137. [PubMed: 22172100]

Walia B, Satija N, Tripathi RP, Gangenahalli GU, 2012. Induced pluripotent stem cells: fundamentals and applications of the reprogramming process and its ramifications on regenerative medicine. Stem Cell Rev. Reports 8, 100–115. 10.1007/s12015-011-9279-x.

Wang W, Yang J, Liu H, Lu D, Chen X, Zenonos Z, Campos LS, Rad R, Guo G, Zhang S, Bradley A, Liu P, 2011. Rapid and efficient reprogramming of somatic cells to induced pluripotent stem cells by retinoic acid receptor gamma and liver receptor homolog 1. Proc. Natl. Acad. Sci 108, 18283–18288. 10.1073/pnas.1100893108. [PubMed: 21990348]

Wolff SC, Kedziora KM, Dumitru R, Dungee CD, Zikry TM, Beltran AS, Haggerty RA, Cheng J, Redick MA, Purvis JE, 2018. Inheritance of OCT4 predetermines fate choice in human embryonic stem cells. Mol. Syst. Biol 14, e8140. 10.15252/msb.20178140. [PubMed: 30177503]

Wood TE, Dalili S, Simpson CD, Sukhai MA, Hurren R, Anyiwe K, Mao X, Suarez Saiz F, Gronda M, Eberhard Y, MacLean N, Ketela T, Reed JC, Moffat J, Minden MD, Batey RA, Schimmer AD, 2010. Selective inhibition of histone deacetylases sensitizes malignant cells to death receptor ligands. Mol. Cancer Ther 9, 246–256. 10.1158/1535-7163.MCT-09-0495. [PubMed: 20053768]

Yu C, Liu Y, Ma T, Liu K, Xu S, Zhang Y, Liu H, La Russa M, Xie M, Ding S, Qi LS, 2015. Small molecules enhance crispr genome editing in pluripotent stem cells. Cell Stem Cell 16, 142–147. 10.1016/j.stem.2015.01.003. [PubMed: 25658371]

Yuan X, Wan H, Zhao X, Zhu S, Zhou Q, Ding S, 2011. Brief report: combined chemical treatment enables Oct4-induced reprogramming from mouse embryonic fibroblasts. Stem Cells 29, 549–553. 10.1002/stem.594. [PubMed: 21425417]

Zeineddine D, Hammoud AA, Mortada M, Boeuf H, 2014. The Oct4 protein: more than a magic stemness marker. Am J Stem Cells 3, 74–82. [PubMed: 25232507]

Zhou H, Ding S, 2010. Evolution of induced pluripotent stem cell technology. Curr. Opin. Hematol 8, 288. 10.1097/MOH.0b013e328339f2ee.

Zhu S, Li W, Zhou H, Wei W, Ambasudhan R, Lin T, Kim J, Zhang K, Ding S, 2010. Reprogramming of human primary somatic cells by OCT4 and chemical compounds. Cell Stem Cell 7, 651–655. 10.1016/j.stem.2010.11.015. [PubMed: 21112560]

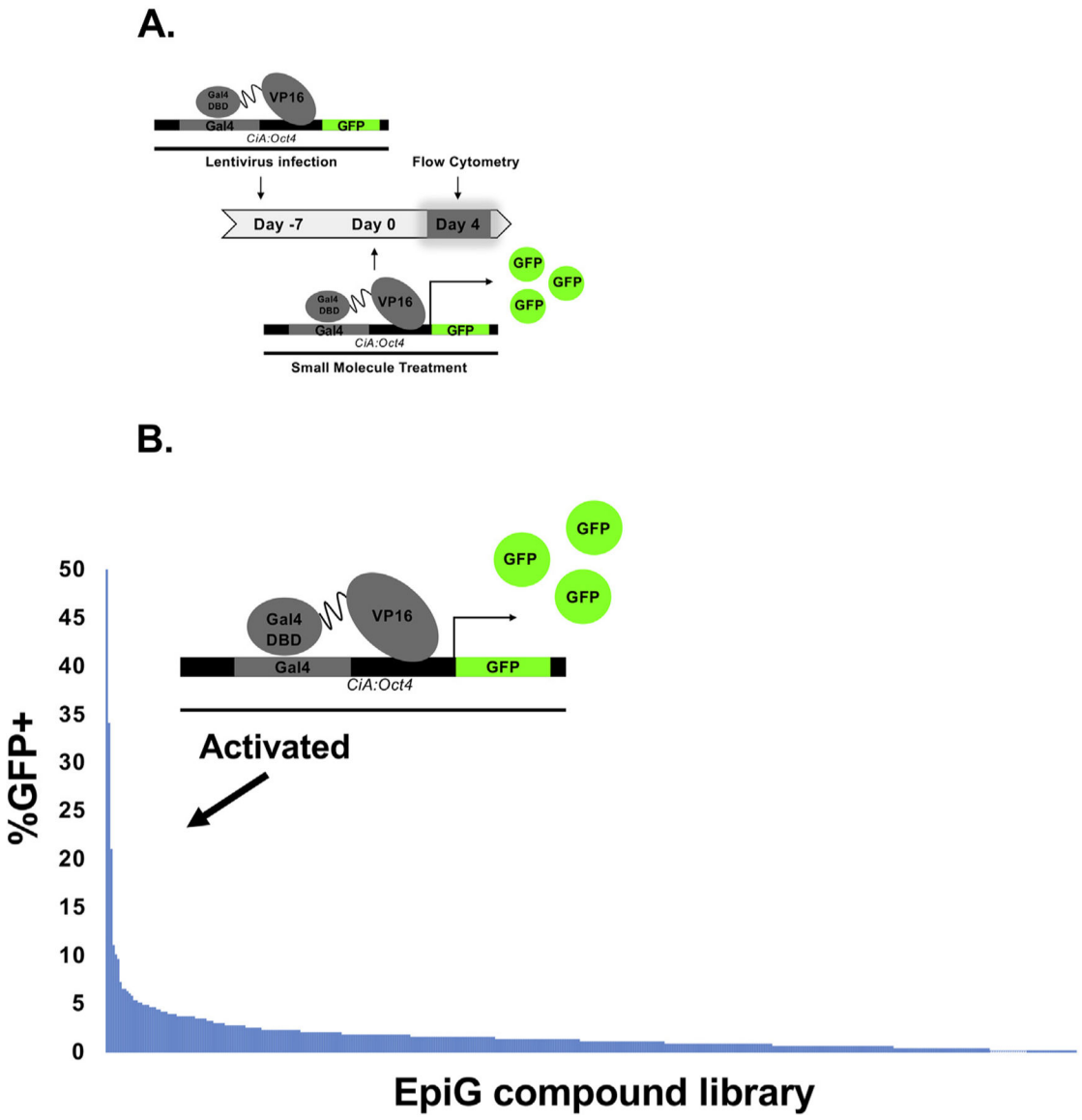

Fig. 1.

Small molecule high throughput screen reveals chemical facilitators of *CiA:Oct4* activation. (A) Schematic representation of experimental timeline. Addition of lentivirus occurred at Day −7. Selection for proper transduction was added on Day −5. Small molecules were added to media on Day 0 and flow cytometry analysis was performed on Day 4. (B) ~960 Small molecules were screened, results represented as %GFP activation after four days of small molecule treatment ordered from highest (left) to lowest (right) percentage of GFP positive cells.

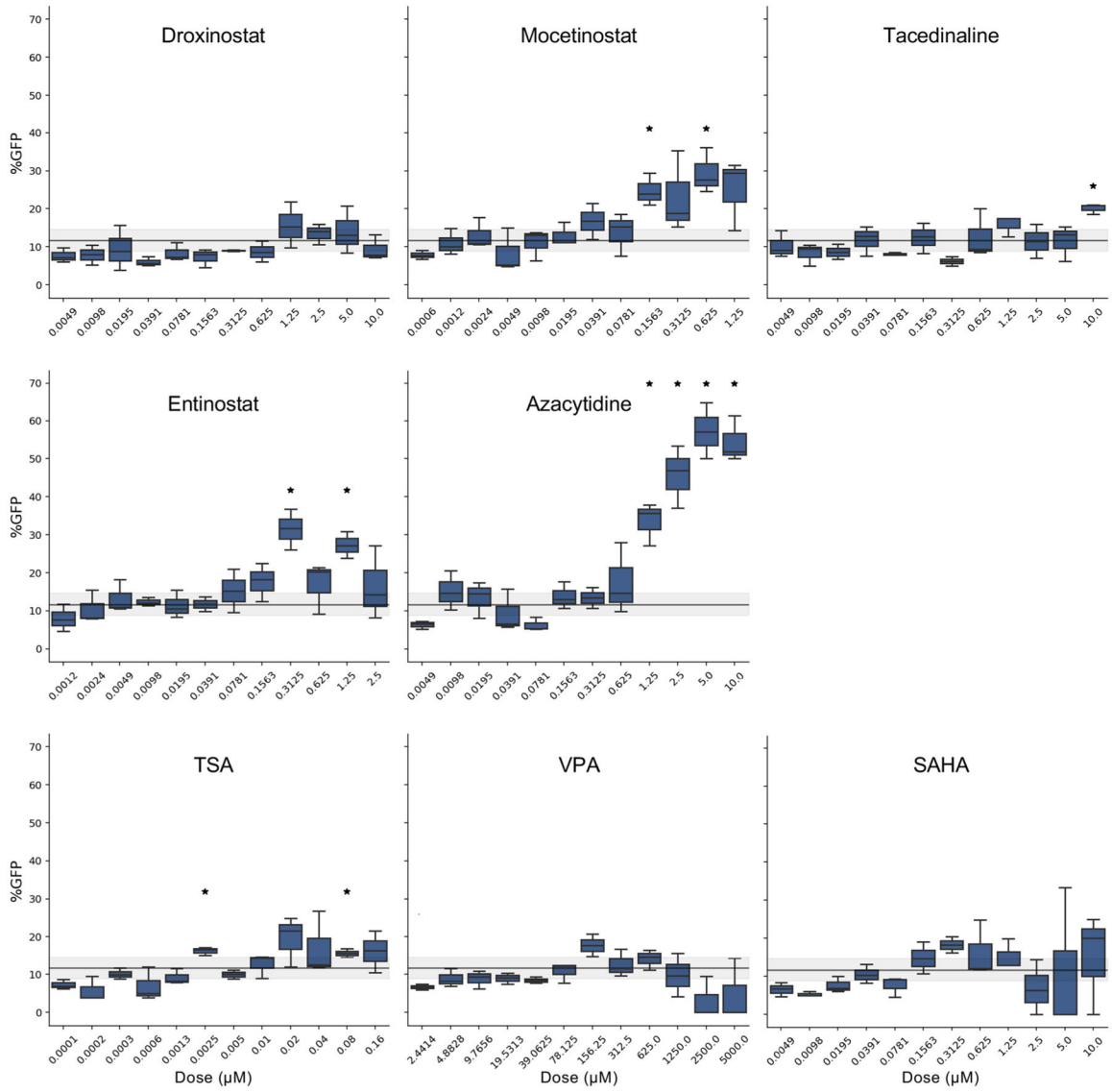

Fig. 2.

Dose response of five selected top hit compounds to triage compounds worth further analysis.(A) Schematic representation of procedural timeline. Lentivirus infection occurred on Day −7. Small molecule was added to cells on Day 0. Flow cytometry analysis was performed on Day 4. (B) Small molecule treatment dose response demonstrates best dosage for small molecule treatment and comparison to well characterized HDACis: TSA, SAHA, and VPA. The control average is shown as gray line and 95% confidence interval is shown as a gray shadow around this line. ($p \leq 0.05$*) Error bars represent standard deviation. The control average activation is represented with a gray line and the surrounding gray shadow represents the 95% confidence interval of the control average.

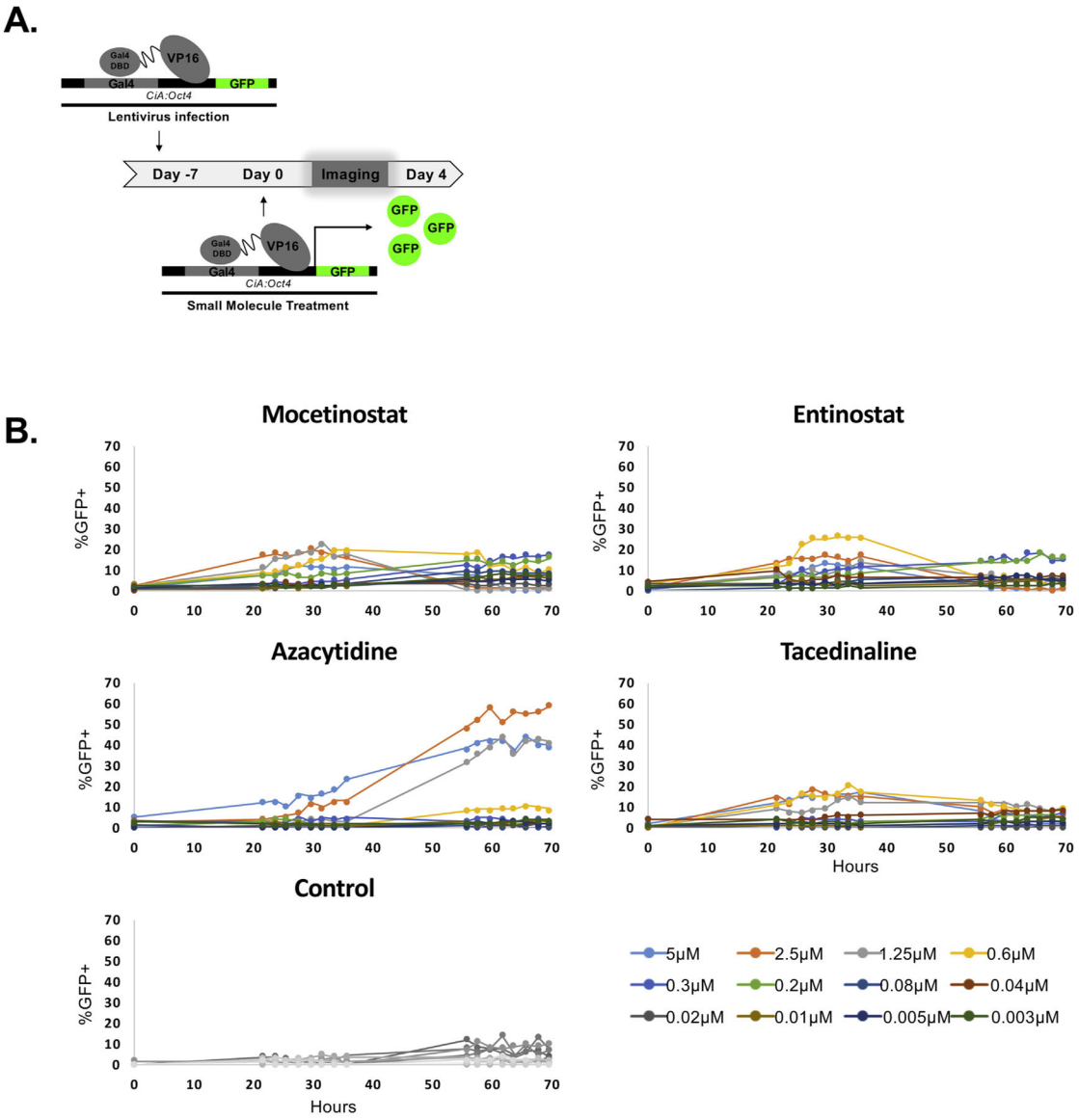

Fig. 3.

Live cell imaging of *CiA:Oct4* during recruitment transcriptional activator and treatment of indicated small molecule. (A) Schematic representation of procedural timeline. Cells were infected with Lentivirus on day −7. Small Molecules were added to cells at the indicated doses on day 0 and imaged at the indicated times until Day 4 (B) Time-lapse imaging reveals dynamics of HDACi facilitated *CiA:Oct4* activation vs. DNTMi facilitated *CiA:Oct4* activation. High content time-lapse imaging data was collected at the indicated times from hours 0 to 70. Analysis was performed using GE Cell Developer to count GFP+ nuclei and mC+ nuclei over time. % GFP+ cells were calculated by dividing GFP counts by mC counts over time (See Supplementary Figure 4 for image example).

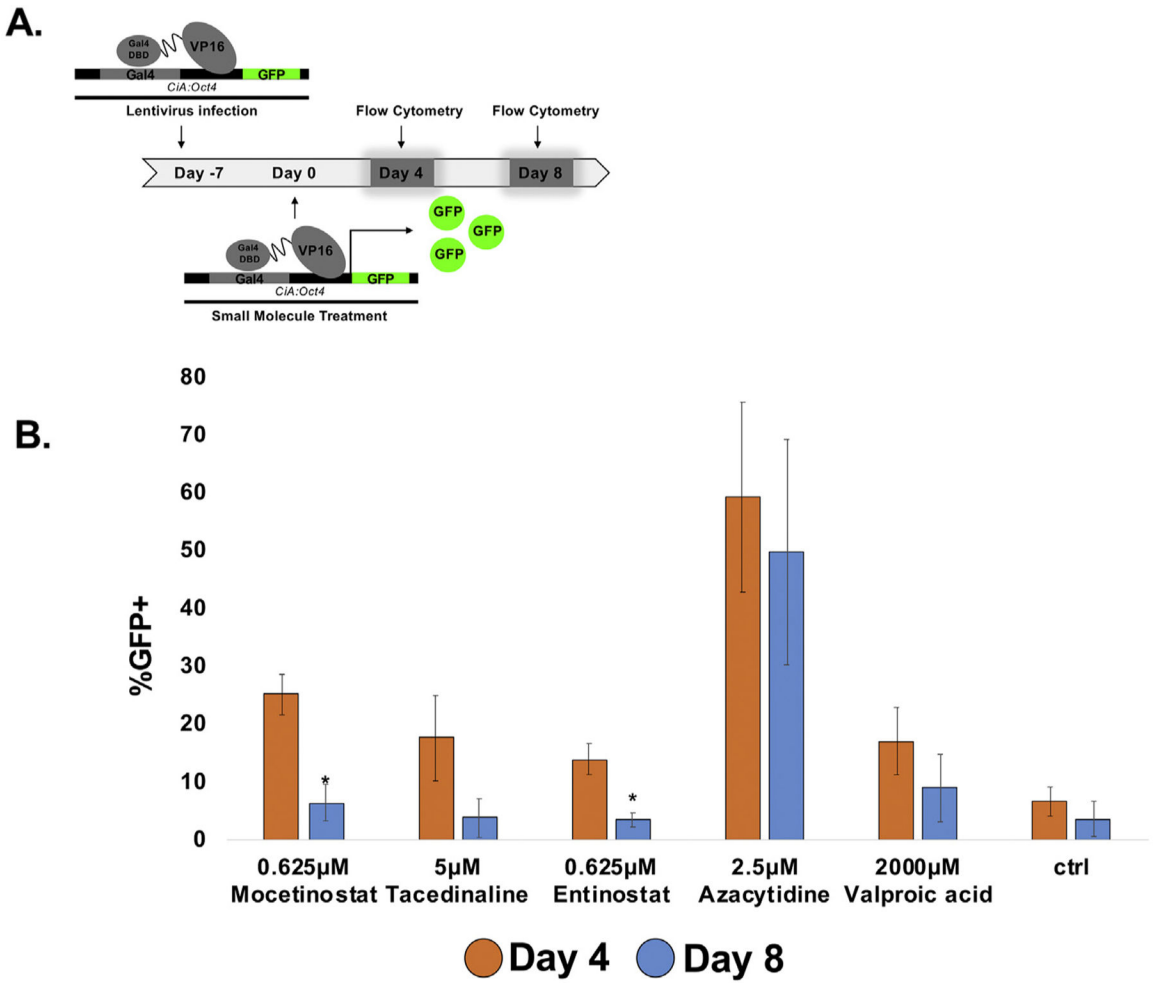

Fig. 4.

Flow cytometry analysis of memory of small molecule facilitation of *CiA:Oct4* activation before and after a 4 day washout. (A) Schematic representation of procedural timeline. Cell infection occurred on Day −7. Cells were treated with small molecules on Day 0 through Day 4. Flow cytometry was performed on the cells on Day 4. Small molecule treatment was released on Day 4. Flow cytometry was performed 4 days after release, on day 8. (B) DNMTi results in long-term gene activation while HDACi has short-term gene activation demonstrated by small molecule release. Day 4 in orange shows percent GFP positive cells identified by flow cytometry of cells treated with the indicated small molecule. Day 8 in blue shows percent GFP cells identified by flow cytometry of cells treated with the indicated small molecule than released from small molecule treatment for four days. ($p \leq 0.05$*). Error bars represent standard deviation.

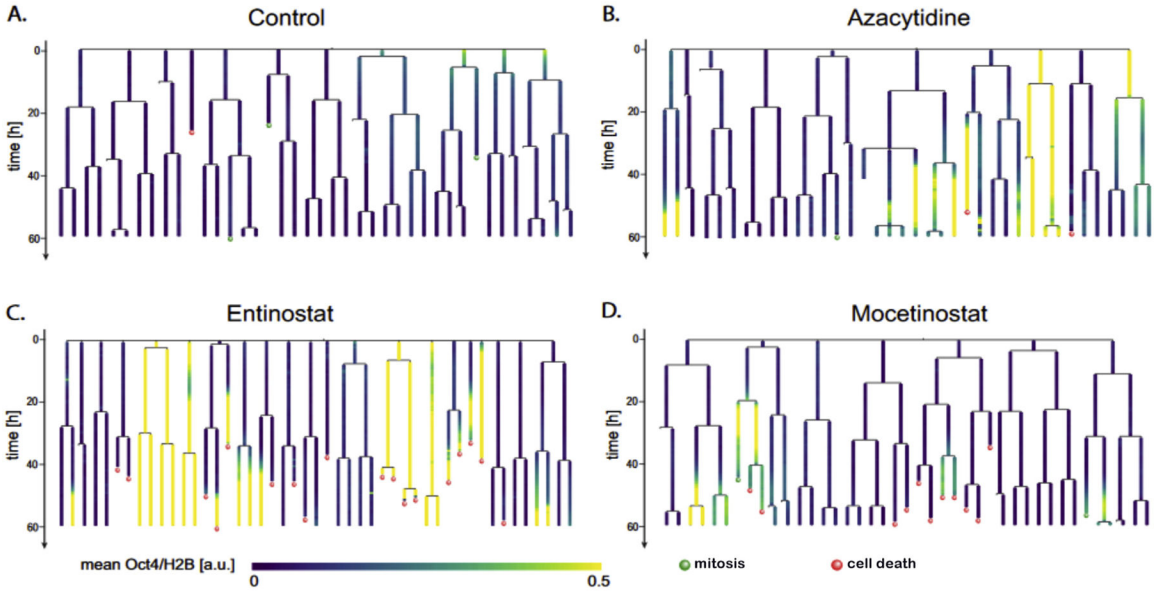

Fig. 5.

Single cell traces from a time-lapse imaging experiment showing GFP(Oct4)/H2B-mCherry ratio of cell families growing in different conditions: A. control; B. Azacytidine; C. Entinostat; D. Mocetinostat. Green dots indicate mitosis of cells which offspring was not tracked. Red dots indicate cell death. Cell death rate (see M& M): control - 2.5% (1/40); Azacytidine 5% (2/38); Entinostat – 38% (18/47); Mocetinostat – 27% (11/41). Total duration of the experiments 60 hours.

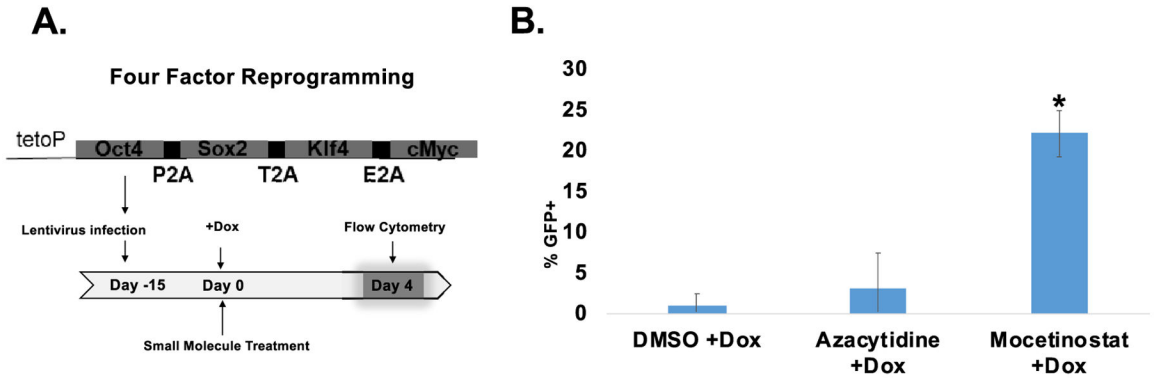

Fig. 6.

Mocetinostat treatment increases transcription factor reprogramming. (A) Schematic representation of timeline. Cells were infected on Day −15, Cells were treated with small molecules on Day 0 and flow cytometry was performed on Day 4 (B) Mocetinostat treated cells demonstrated increased *Oct4* activation during transcription factor reprogramming with polycistronic vector for *Oct4*, Sox2, Klf4, and cMyc. ($p \leq 0.05$*) Error bars represent standard deviation and p-values are representative comparison to DMSO (+Dox).